HS2ST1-dependent signaling pathways determine breast cancer cell viability, matrix interactions, and invasive behavior

Archana Vijaya Kumar, Stéphane Brézillon, Valérie Untereiner, Ganesh Sockalingum, Sampath Kumar Katakam, Hossam Taha Mohamed, Björn Kemper, Burkhard Greve, Benedikt Mohr, Sherif Abdelaziz Ibrahim, et al.

▶ **To cite this version:**

Archana Vijaya Kumar, Stéphane Brézillon, Valérie Untereiner, Ganesh Sockalingum, Sampath Kumar Katakam, et al.. HS2ST1-dependent signaling pathways determine breast cancer cell viability, matrix interactions, and invasive behavior. Cancer Science, 2020, 111 (8), pp.2907-2922. 10.1111/cas.14539 . hal-02986569

HAL Id: hal-02986569

https://hal.univ-reims.fr/hal-02986569v1

Submitted on 17 Nov 2020

HAL is a multi-disciplinary open access archive for the deposit and dissemination of scientific research documents, whether they are published or not. The documents may come from teaching and research institutions in France or abroad, or from public or private research centers.

L'archive ouverte pluridisciplinaire **HAL**, est destinée au dépôt et à la diffusion de documents scientifiques de niveau recherche, publiés ou non, émanant des établissements d'enseignement et de recherche français ou étrangers, des laboratoires publics ou privés.

Distributed under a Creative Commons Attribution - NonCommercial - NoDerivatives 4.0 International License

Received: 21 January 2020 | Revised: 10 June 2020 | Accepted: 12 June 2020

DOI: 10.1111/cas.14539

ORIGINAL ARTICLE

Cancer Science WILEY

HS2ST1-dependent signaling pathways determine breast cancer cell viability, matrix interactions, and invasive behavior

Archana Vijaya Kumar[1] | Stéphane Brézillon[2] | Valérie Untereiner[3] | Ganesh Dhruvananda Sockalingum[4] | Sampath Kumar Katakam[1] | Hossam Taha Mohamed[2,5,6] | Björn Kemper[7] | Burkhard Greve[8] | Benedikt Mohr[1] | Sherif Abdelaziz Ibrahim[5] | Francisco M. Goycoolea[9] | Ludwig Kiesel[1] | Mauro S.G. Pavão[10] | Juliana M. Motta[10] | Martin Götte[1]

[1]Department of Gynecology and Obstetrics, Münster University Hospital, Münster, Germany

[2]CNRS, MEDyC UMR 7369, UFR de Médecine, Université de Reims Champagne-Ardenne, Reims, France

[3]Université de Reims Champagne-Ardenne, PICT, Reims, France

[4]Université de Reims Champagne-Ardenne, BioSpecT EA7506, Reims, France

[5]Department of Zoology, Faculty of Science, Cairo University, Giza, Egypt

[6]Faculty of Biotechnology, October University for Modern Sciences and Arts, Giza, Egypt

[7]Biomedical Technology Center of the Medical Faculty, University of Münster, Münster, Germany

[8]Department of Radiotherapy – Radiooncology, University Hospital Münster, Münster, Germany

[9]School of Food Science and Nutrition, University of Leeds, Leeds, UK

[10]Instituto de Bioquímica Médica Leopoldo de Meis, Universidade Federal do Rio de Janeiro, Rio de Janeiro, Brazil

Correspondence
Martin Götte, Department of Gynecology and Obstetrics, Münster University Hospital, Domagkstrasse 11, 48149 Münster, Germany.
Email: mgotte@uni-muenster.de

Funding information
Deutsche Forschungsgemeinschaft, Grant/Award Number: GRK 1549; Deutscher Akademischer Austauschdienst, Grant/Award Number: PROBRAL 54387857; WWU fellowship of the University of Münster

Abstract

Heparan sulfate proteoglycans (HSPGs) act as signaling co-receptors by interaction of their sulfated glycosaminoglycan chains with numerous signaling molecules. In breast cancer, the function of heparan sulfate 2-*O*-sulfotransferase (*HS2ST1*), the enzyme mediating 2-*O*-sulfation of HS, is largely unknown. Hence, a comparative study on the functional consequences of *HS2ST1* overexpression and siRNA knockdown was performed in the breast cancer cell lines MCF-7 and MDA-MB-231. *HS2ST1* overexpression inhibited Matrigel invasion, while its knockdown reversed the phenotype. Likewise, cell motility and adhesion to fibronectin and laminin were affected by altered *HS2ST1* expression. Phosphokinase array screening revealed a general decrease in signaling via multiple pathways. Fluorescent ligand binding studies revealed altered binding of fibroblast growth factor 2 (FGF-2) to *HS2ST1*-expressing cells compared with control cells. *HS2ST1*-overexpressing cells showed reduced MAPK signaling responses to FGF-2, and altered expression of epidermal growth factor receptor (EGFR), E-cadherin, Wnt-7a, and Tcf4. The increased viability of *HS2ST1*-depleted cells was reduced to control levels by pharmacological MAPK pathway inhibition.

*Juliana M. Motta and Martin Götte are shared senior authors of this study.

This is an open access article under the terms of the Creative Commons Attribution-NonCommercial-NoDerivs License, which permits use and distribution in any medium, provided the original work is properly cited, the use is non-commercial and no modifications or adaptations are made.
© 2020 The Authors. *Cancer Science* published by John Wiley & Sons Australia, Ltd on behalf of Japanese Cancer Association.

Moreover, MAPK inhibitors generated a phenocopy of the *HS2ST1*-dependent delay in scratch wound repair. In conclusion, *HS2ST1* modulation of breast cancer cell invasiveness is a compound effect of altered E-cadherin and EGFR expression, leading to altered signaling via MAPK and additional pathways.

KEYWORDS
2-O-sulfotransferase, breast cancer, heparan sulfate, MAPK signaling pathway, proteoglycan

1 | INTRODUCTION

Heparan sulfate proteoglycans (HSPGs) are glycoproteins of cell surfaces and the extracellular matrix (ECM) carrying unbranched polysaccharide chains called glycosaminoglycans (GAGs).[1-3] HS GAGs contain repetitive disaccharide units comprised of alternating uronic acids and *N*-acetyl-glucosamine that are extensively modified by sulfation.[1-3] HSPGs have crucial regulatory roles in normal physiology and pathophysiological conditions, like inflammation, immunomodulation, and tumor onset and progression.[3-5] Cell surface HSPGs immobilize and regulate ECM turnover, providing cytokines, growth factors, and other signaling molecules to receptors on cancer cells to support growth, survival, motility, and angiogenesis.[1,2,6] They also cooperate with integrins and adhesion receptors to facilitate cell-ECM attachment, cell-cell interactions, and cell motility.[2,7]

HS biosynthesis begins in the Golgi apparatus with the attachment of a linker tetrasaccharide to a core protein serine residue. A backbone of repeated *N*-acetyl glucosamine (GlcNAc) linked to D-glucuronic acid (GlcA) is synthesized on this linker and extended by the glycosyltranferases-EXT1 and EXT2.[2,8] Subsequent modification includes *N*-deacetylation and *N*-sulfation of some GlcNAc units to *N*-sulfated glucosamine (GlcNS), catalyzed by *N*-deacetylase sulfotransferases (NDSTs), epimerization of some GlcA to iduronate (IdoA) catalyzed by C5-epimerase, followed by 2-*O*-sulfation of uronate residues catalyzed by HS 2-*O* sulfotransferase (*HS2ST1*, *2-OST*).[1,2] 6-*O*-Sulfation of GlcNAc/GlcNS is catalyzed by HS 6-*O* sulfotransferases, whereas rare 3-*O*-sulfation modifications of the GlcNAc or GlcNS units are mediated by 3-*O*-sulfotransferases.[1,9]

Cells normally try to maintain the net overall sulfation profile constant.[10] A change in sulfation status at one ring position can be compensated by sulfation at other positions by tightly regulated activities of HS-modifying enzymes in the postulated GAGosome.[10-13] Key structural determinants of HS interaction with cytokines are the degree, pattern and clustering of sulfated disaccharides along the HS chain,[9,14-17] which influence the binding ability of HSPG co-receptors to the ligands.

The present study focuses on the role of the HS biosynthetic enzyme *HS2ST1* in breast cancer progression.[12,18,19] Previous studies in model organisms have demonstrated a role for 2-*O*-sulfation in cell migration and differentiation through unknown pathways.[20,21] Although HSPGs play an important role in malignancies,[22-24] very little is known about the specific functional role of *HS2ST1* in cancer pathogenesis. We show that *HS2ST1* upregulation in breast cancer cell lines reduces their migratory and invasive behavior due to a decrease in epidermal growth factor receptor (EGFR) and E-cadherin expression and overall phosphokinase signaling. Phenotypic effects are associated with altered binding of growth factors to 2-*O* sulfated HS, and depend on MAPK signaling. These results demonstrate for the first time that increased *HS2ST1* expression controls the invasiveness of breast cancer cells.

2 | MATERIALS AND METHODS

2.1 | Materials

Medium, fetal calf serum (FCS) and tissue culture supplies were from Gibco BRL. Unless stated otherwise, all chemicals were from Sigma.

2.2 | Cell culture

MCF-7 and MDA-MB-231 breast cancer cells were purchased from ATCC/LGC Promochem. Cells were stably transfected as described[25] with a pcDNA3.1 control plasmid (Invitrogen) or a plasmid allowing for expression of the open reading frame (1104 bp) of human *HS2ST1* (NCBI Reference Sequence: NM_012262) in the vector pReceiver-M02 under the control of the cytomegalovirus (CMV) promoter (RZPD/ImaGenes). MDA-MB-231 cells were maintained in Dulbecco's Modified Eagle Medium (DMEM) containing 10% FCS, 1% glutamine, 1% penicillin/streptomycin and 800 μg/mL G418 in a humidified atmosphere of 7.5% CO_2 in air at 37°C. MCF-7 cells were cultured in RPMI-1640 medium containing 10% FCS, 1% glutamine, 1% penicillin/streptomycin and 800 μg/mL G418 in a humidified atmosphere of 5% CO_2 in air at 37°C. In some experiments, 10 μmol/L U0126 (Cell Signaling Technologies) was used to inhibit the MAPK pathway.

2.3 | *HS2ST1*siRNA knockdown

siRNA knockdown was performed using Dharmafect (Dharmacon) and 20 nmol/L validated silencer select siRNA #18569, targeting exon 4 of *HS2ST1*, siRNA #18570, targeting exon 2 of *HS2ST1*, and negative control siRNA #1 (Ambion) according to the manufacturer's instructions. Cellular phenotypes of siRNA-treated cells were

analyzed after 48 h (PCR) or 72 h (protein-based assays, functional assays), respectively.

2.4 | Disaccharide analysis of glycosaminoglycans

GAG isolation was performed from cell pellets as described earlier[26] except for elution of DEAE columns with 2 mol/L NaCl followed by desalting on PD MiniTrap™ G-25 columns (GE Healthcare). GAGs were digested with 50 mU of chondroitinase ABC (Seikagaku) and 10% of the total sample directly analyzed by reverse-phase ion-pairing high-performance chromatography (RPIP-HPLC). The remaining 90% were reapplied to a DEAE column and eluted to remove CS-disaccharides. The eluted HS pool was split into 2 equal aliquots and one incubated without, the other with, a mixture of 0.4 mU each of heparin lyases I, II and III (IBEX). Disaccharide separation was performed by RPIP-HPLC as described.[26] Peaks were identified by co-elution with standard CS and HS disaccharides.

2.5 | Cell viability assay

Cell viability was evaluated by MTT (3-(4,5-dimethylthiazol-2-yl)-2,5-diphenyltetrazolium bromide) assay essentially as previously described.[27] Here, 5000 cells were seeded in quadruplets into 96-well plates and cultured for 24, 48, or 72 h, respectively. Afterwards, 4 h of incubation in the presence of 5 mg/mL MTT followed. Cells were lysed by addition of an equal volume of 10% sodium dodecyl sulfate (SDS) in 50% *N,N*-dimethylformamide, pH 4.7, for 16 h, and optical density measurement at 595 nm was performed using a microplate reader. Cell viability data are shown as percentage viability of vector/control siRNA-treated cells.

2.6 | Apoptosis assay

Apoptotic cells were identified by flow cytometry using the Annexin V test kit (Becton Dickinson), based on their property of binding fluorescently labeled annexin V as a result of apoptosis-related membrane inversions. Cells were counterstained with propidium iodide to identify late apoptotic/necrotic cells. Fluorescence emission was measured at 527 and 675 nm on a flow cytometer (CyFlow Space, Partec).

2.7 | Invasion assay

BioCoat Matrigel Invasion Chamber (BD Biosciences) assays were performed exactly as described previously.[25,27] Briefly, 25 000 cells were seeded into invasion filters (BD Biosciences) in a 24-well plate format and incubated for another 24 h. Invasion was induced by addition of serum-free medium to the upper chamber and of 10% FCS-containing medium as chemoattractant to the bottom chamber of the invasion chamber for another 24 h (MDA-MB-231) or 48 h (MCF-7), respectively, resulting in transmigration of the cells through the basement-membrane-like extracellular matrix. Cells in the upper chamber were removed with a cotton swab, and cells on the lower surface were fixed and stained with Diff-Quik dye (Medion). Excised and mounted filter membranes were photographed using a Zeiss Axiovert microscope (Zeiss) at ×100 magnification. Relative invasiveness was expressed as percentage of the HS2ST1-overexpressing or siRNA-treated cells compared with vector/control siRNA-treated cells ($n > 3$).

2.8 | Scratch motility assay

Scratch motility assays were performed as previously described.[27] Confluent cell monolayers were wounded by scraping once horizontally and vertically with a 100 μL pipette tip. Closing of the scratch wound was monitored by Nomarski contrast light microscopy and documented with a Zeiss Axiophot camera (Zeiss) immediately and 6 h after wounding. Zeiss Axiovision software (Zeiss) was used to calculate the cell-free wounded area. Data are shown as percentage of the cell-free area of *HS2ST1*-manipulated cells compared with controls.

2.9 | Migration assay and digital holographic microscopy

An inverted microscope (iMIC, Till Photonics) with an attached digital holographic microscopy (DHM) module[28] and an incubator (Solent Scientific Ltd.) for stabilized temperature were used for bright-field imaging and quantitative digital holographic phase-contrast imaging of control and *HS2ST1*-overexpressing MDA-MB-231 cells seeded on laminin-coated Petri dishes. The coherent light source for the recording of digital holograms was a frequency-doubled neodymium-doped yttrium aluminum garnet (Nd:YAG) laser (Compass 315 M-100, Coherent, $\lambda = 532$ nm). Experiments were performed in μ-dishes (ibidi GmbH) seeded with 3×10^4 cells. Digital holograms of single cells were recorded continuously every 3 min. Digitally captured hologram reconstruction was performed by spatial phase shifting reconstruction.[29] For DHM, the cells were cultured in HEPES-buffered DMEM. Three independent single cell analyses were performed and representative measurements are shown in the results. Migratory behavior of cells was analyzed by automated cell tracking.[30]

2.10 | Adhesion assay

Here, 96-well plates were coated with 10 μg/mL fibronectin or 50 μg/mL laminin or 10 μg/mL BSA (negative control) for 16 h at 4°C and washed twice with wash solution (0.1% BSA in DMEM), followed by blocking of nonspecific binding with 0.5% BSA in DMEM at room temperature. Adhesion of 2.5×10^4 cells/well was quantified

using a photometric methylene blue staining based method as previously described.[7] Cells were released with 2 mmol/L EDTA in PBS, washed twice, and resuspended in blocking solution prior to incubation with the coated wells for 1 h at 37°C. Nonadherent cells were removed by 3 washes with PBS. Following fixation of attached cells with 3.7% NaCl/PBS-buffered formaldehyde for 30 min, cells were stained with 1% methylene blue in 0.01% borate buffer (pH 8.5) for 30 min. Following 4 washes with borate buffer, the cells were lysed in ethanol/0.1 mol/L HCl (1:1), and the released stain was quantified in a Softmax Microplate reader (Molecular Devices) at 620 nm. Data are expressed as percentage of *HS2ST1*-manipulated cell values compared with control cells.

2.11 | Quantitative real-time PCR

Total cellular RNA was isolated using RNA-OLS (OMNI Life Science) and reverse transcribed (Advantage First strand cDNA synthesis kit; Fermentas). qPCR and melting curve analysis were performed using Qiagen QuantiTect SYBR Green PCR kit in a LightCycler. Expression of additional mRNAs was analyzed using TaqMan probes on an ABI PRISM 7300 Sequence Detection System as described previously using the $2^{-\Delta\Delta Ct}$ method after normalization to 18S rRNA.[27] The following TaqMan probes were used (see also lifetechnologies.com): 18S rRNA: hs 99999901_s1; EGFR: hs 00193306_m1; HS2ST1: hs_00202138_m1; Wnt 7a: hs 01114990_m1.

2.12 | Western blotting

Western blotting was performed as previously described.[7] Briefly, cells were lysed in modified RIPA buffer with proteinase inhibitors. 50 μg of protein per lane were separated on 10% gels, and electrotransferred to Hybond nitrocellulose membranes (Amersham, Pharmacia Biotech). For antibody incubations, the membranes were blocked with 5% skimmed milk in 0.1% TBS-Tween (TBST) for 1 h at room temperature, followed by incubation with the primary antibody overnight at 4°C. Antibodies and dilutions are listed in Table 1. After washing in TBST buffer 3 times, the membranes were incubated for 30 min at room temperature with horseradish peroxidase-conjugated secondary antibodies in blocking buffer. The membranes were washed and treated with enhanced chemiluminescence detection reagents (Amersham Pharmacia Biotech) for 1 min and exposed to Hyperfilm-ECL. For detection of the total forms of phosphorylated proteins, and for detection of the housekeeping control protein tubulin, membranes were stripped with 0.2 mol/L glycine buffer (pH 2.5), washed, reincubated with primary antibody, and subjected to the procedure described above.

2.13 | Phosphokinase array

Human phosphokinase array was performed following manufacturer's instructions (R&D Systems). 300 μg of protein from control and *HS2ST1*-overexpressing cells was analyzed in a panel of phosphorylation profiles of kinases.

TABLE 1 Antibodies used in this study

Antibody	Working dilution	Manufacturer
Rabbit polyclonal anti-phospho-Thr202/Tyr204 p44/42 MAPK	1:1000	Cell Signalling
Rabbit polyclonal anti-p44/42 MAPK	1:1000	Cell Signalling
Mouse anti-human E-cadherin, clone 36	1:1000	Becton and Dickinson Biosciences
Rabbit polyclonal anti-EGFR	1:1000	Cell Signalling
Rabbit monoclonal anti-human TCF4	1:1000	Cell Signalling
Rabbit polyclonal anti-HS2ST1	1:1000	Cell Signalling
Rabbit polyclonal anti-phosphor-Thr180/Tyr182 p38 MAPK	1:1000	Cell Signalling
Rabbit polyclonal anti-p38 MAPK	1:1000	Cell Signalling
Mouse anti-human α-Tubulin, clone B-5-1-2	1:4000	Sigma-Aldrich
Horseradish peroxidase-conjugated goat-anti-mouse IgG	1:10 000	Merck-Millipore
Horseradish peroxidase-conjugated goat-anti-rabbit IgG	1:2000	Merck-Millipore
Horseradish peroxidase-conjugated rabbit-anti-goat IgG	1:5000	Merck-Millipore

2.14 | Analysis of biotinylated FGF-2 binding by flow cytometry

Binding of basic fibroblast factor (FGF-2) to 4×10^6 EDTA-detached cells/mL was analyzed by flow cytometry employing Fluorokine^R Biotinylated human FGF-2 and avidin-FITC reagent (R&D Systems) according to the manufacturer's instructions.

2.15 | Heparan sulfate purification from cells for Fourier transform infrared (FTIR) analysis

Here, ~2.5×10^7 cells per sample were washed in PBS, scraped from the flasks, pelleted and lyophilized. The lyophilized cell pellets were separately suspended in 2 mL of 0.1 mol/L sodium acetate buffer (pH 5.5) containing 1% of papain, 5 mmol/L EDTA and 5 mmol/L cysteine and incubated at 60°C overnight. This was then centrifuged at 2000 *g* for 10 min at room temperature, the supernatant was separated. The clear supernatants from different samples were ethanol precipitated and suspended in 0.1 mol/L NaCl. The solution was applied on a DEAE column equilibrated with sodium phosphate buffer (pH 6.0) containing 0.15 mol/L NaCl. Fractions were eluted with 1.0 mol/L NaCl in the same buffer, desalted with HiTrap™

desalting column, lyophilized, and resuspended in 15 μL 0.03 mol/L acetate buffer (pH 7.0) with 1.0 mU/μL chondroitin ABC (in 10 μL cABC buffer, pH 8.0) to degrade chondroitin sulfate and hyaluronan. The mixture was incubated at 37°C overnight, lyophilized and the enzymatic reaction was inactivated at 96°C for 2 min before freeze drying. Samples were resuspended in Milli-Q water to load onto the HPLC for separation of HS.

2.16 | Extraction of total GAGs from conditioned medium

Cells underwent starvation in growth medium without serum for 24 h at 37°C with 5% CO_2 in air. Then, 10 mL of conditioned medium (CM) were centrifuged to remove cell debris. CM supernatants were concentrated using a Vivaspin™ column with a 10 000 Da MWCO (GE Healthcare Bio-Sciences AB), and incubated overnight at 37°C with a pronase (Cat. No. P8811-1G, Sigma-Aldrich) to digest all proteins. Proteinase deactivation was performed by addition of NaCl (50 nmol/L) and incubation at 100°C for 1 min. After cooling, centrifugation was performed to pellet digested proteins. GAGs were precipitated from the supernatant by addition of saturated sodium acetate and incubation at 4°C for 3 h. Precipitated GAGs were air-dried and resuspended in sterile distilled water. For each cell line, 3 independent biological replicates were analyzed.

2.17 | FTIR spectroscopy of extracted GAGs

Here, 5 μL of resuspended extracted GAGs (1 μg/μL) were deposited in triplicate onto a high- throughput 384-well silicon plate, air-dried, and analyzed with a high-throughput screening HTS-XT extension coupled to a Tensor 27 FTIR spectrometer (Bruker Optics GmbH). The FTIR acquisitions of the samples were performed in transmission mode, in the spectral range 4000-400 cm^{-1}, at a spectral resolution of 4 cm^{-1} with 64 scans. Before each sample measurement, the silicon plate background was recorded and automatically removed from the sample signal. One spectrum was obtained from each well. Acquisition and pre-processing were performed with the OPUS software (Version 6.0, Bruker Optics).

2.18 | Spectral data pre-processing and analysis

Before pre-processing, some spectra were discarded after spectral quality test. For FTIR spectral analysis, a baseline correction was performed and a second derivative was calculated to increase the differences between spectra. A vector normalization was applied for spectral comparison. Then, data were processed with multivariate statistical exploratory techniques like hierarchical cluster analysis (HCA) and principal component analysis (PCA). These clustering methods based on distance calculation and variance analysis respectively, allowed for analysis how spectra group together in an unsupervised way. These 2 analyses were performed in the 1350-900 cm^{-1} spectral range. The complete workflow for GAGs analysis by FTIR high-throughput spectroscopy has been reported previously.[31]

2.19 | Statistical analysis

Data were expressed as mean ± SEM or SD, as indicated. Statistical analysis was performed using the Sigma Stat 3.1 software (Systat Software). An unpaired *t* test was used when groups passed the normality test, otherwise, the Mann-Whitney *U* test was used. A two-sided *P*-value < .05 was considered statistically significant.

3 | RESULTS

3.1 | Confirmation of stable overexpression and transient siRNA knockdown of *HS2ST1*

To study the functional impact of increased *HS2ST1* expression, the metastatic triple-negative cell line MDA-MB-231 and the less dedifferentiated and less invasive hormone-receptor-positive cell line MCF-7 were stably transfected with a control vector and a plasmid overexpressing *HS2ST1* under the control of a strong CMV promoter, respectively. To ensure that the observed phenotypic end points are due to increased *HS2ST1* expression and not to other molecular mechanisms, a complementary transient siRNA knockdown approach was implemented. In addition, key experiments were confirmed using independent overexpressing clones (see Figure S1). qPCR analysis showed an 8-11-fold increase in mRNA expression of *HS2ST1* (Figure 1A and Figure S1A) and up to 90% decrease in its expression upon siRNA knock down (Figure 1B). The change in *HS2ST1* expression was confirmed at the protein level by western blotting (Figure 1C,D).

3.2 | FTIR discrimination of *HS2ST1*-overexpressing cells based on extracted GAGs

Taking into account the specific spectral signatures obtained from standard GAG molecules and GAG mixtures[32,33] and from cells based on their capacity for GAG synthesis,[34] FTIR measurements were undertaken to characterize extracted GAGs from the CM of *HS2ST1*-overexpressing vs control cells. The mean normalized FTIR spectra obtained of extracted GAGs showed differences between MCF-7 and MDA-MB-231 cell lines in the 1800-900 cm^{-1} spectral range. These differences were more visible in the 1350-800 cm^{-1} spectral range (GAGs absorption region). This region was selected for exploratory chemometrics analysis. Moreover, in the 1350-800 cm^{-1} spectral range, extracted GAGs from control and *HS2ST1*-overexpressing MCF-7 or MDA-MB-231 cells could be easily discriminated. HCA and PCA were performed on second derivative spectra in the 1350-800 cm^{-1} spectral range. HCA results displayed

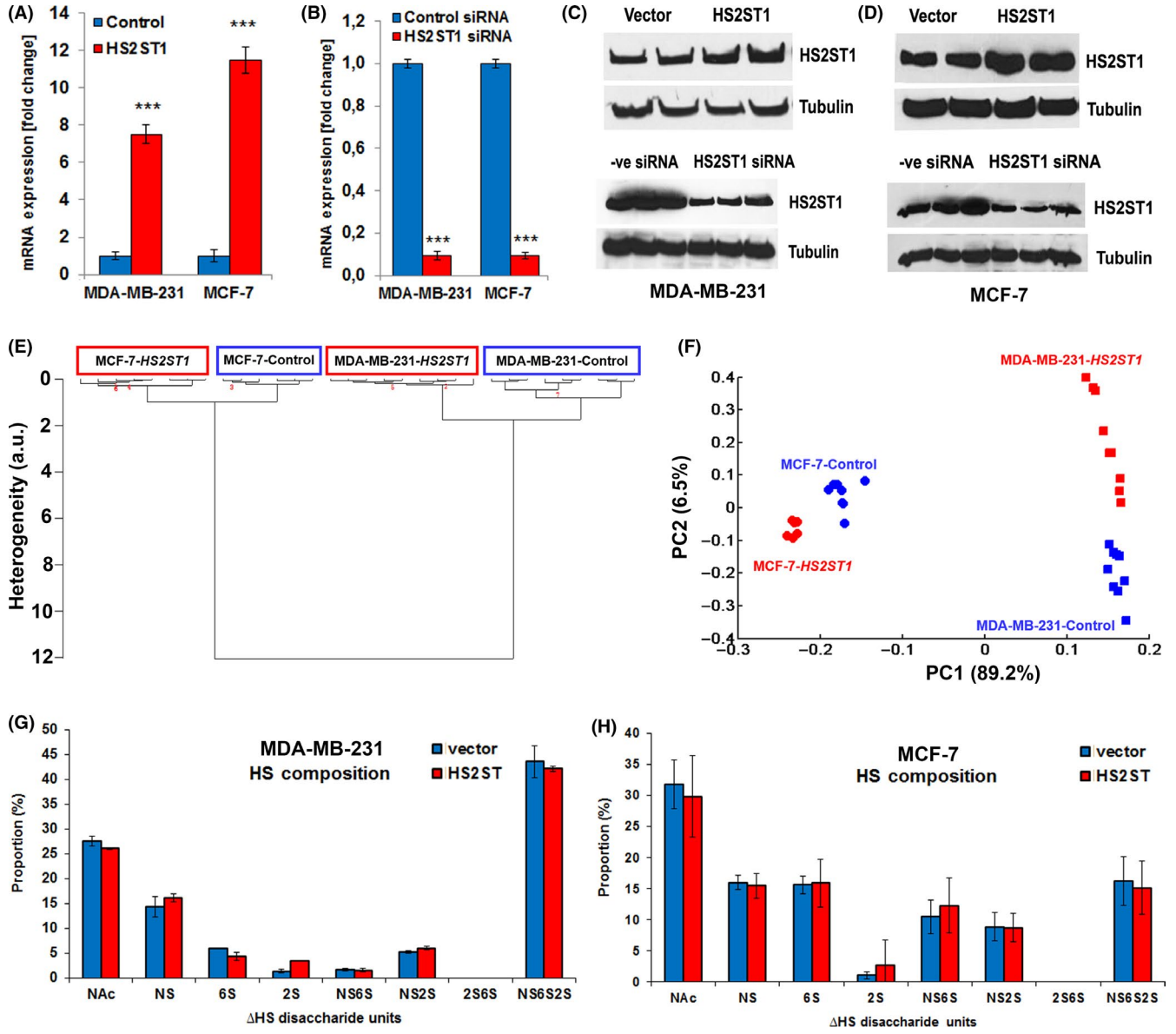

FIGURE 1 Overexpression of *HS2ST1* results in altered FTIR spectra. A, B, qPCR (A, B) and western blotting (C, D) confirm stable transfection (A) and siRNA knockdown (B) of *HS2ST1*in MDA-MB-231 and MCF-7 cells. A, B, N = 9, Error bars = SEM, ***$P < .001$. C, D, Upper panels, plasmid-based overexpression; lower panels, siRNA knockdown. E, Hierarchical cluster analysis of FTIR spectra of GAGs from conditioned medium (CM) of control and *HS2ST1*-overexpressing cells. F, Principal component analysis score plot of FTIR spectra of GAGs extracted from CM of control and HS2ST1-overexpressing cells. E, F, Analysis was performed on second derivative spectra in the 1350-800 cm^{-1} spectral range. G, H, Biochemical RPIP-HPLC characterization of HS disaccharides of *HS2ST1*-transfected cells. Peaks co-eluting with standard disaccharides are labeled as *N*-acetylglucosamine (NAc), *N*-sulfated glucosamine (NS) and sulfate group at indicated position (S). N = 2 independent analyses

in Figure 1E showed that spectra of GAGs extracted from CM of the same cell type were grouped in the same cluster. They exhibited a low degree of heterogeneity, indicating a good reproducibility, and a low intra-group variability, which was sufficient to distinguish between MCF-7 and MDA-MB-231 CM. Moreover, CM from control and *HS2ST1*-transfected cells could be discriminated. To confirm these observations, a second chemometric method based on PCA analysis was carried out. Figure 1F shows the PCA score plot of the CM of each cell type using the first 2 principal components (PCs) carrying the highest explained variance. The first PC (PC1) carried 89.2% of the total variance and allowed a clear separation between CM from MCF-7 and MDA-MB-231 cell lines. These results also showed that PC2, representing 6.5% of the total variance, allowed the separation of CM between control and *HS2ST1*-overexpressing cells. This is clear for MDA-MB-231 cell types while a combination of PC1 and PC2 seemed to be necessary to delineate between MCF-7 cell types. Disaccharide analysis of *HS2ST1*-overexpressing MDA-MB-231 (Figure 1G) and MCF-7 (Figure 1H) cells also revealed a slight increase of 2-*O*-sulfated HS structures compared with their corresponding vector controls.

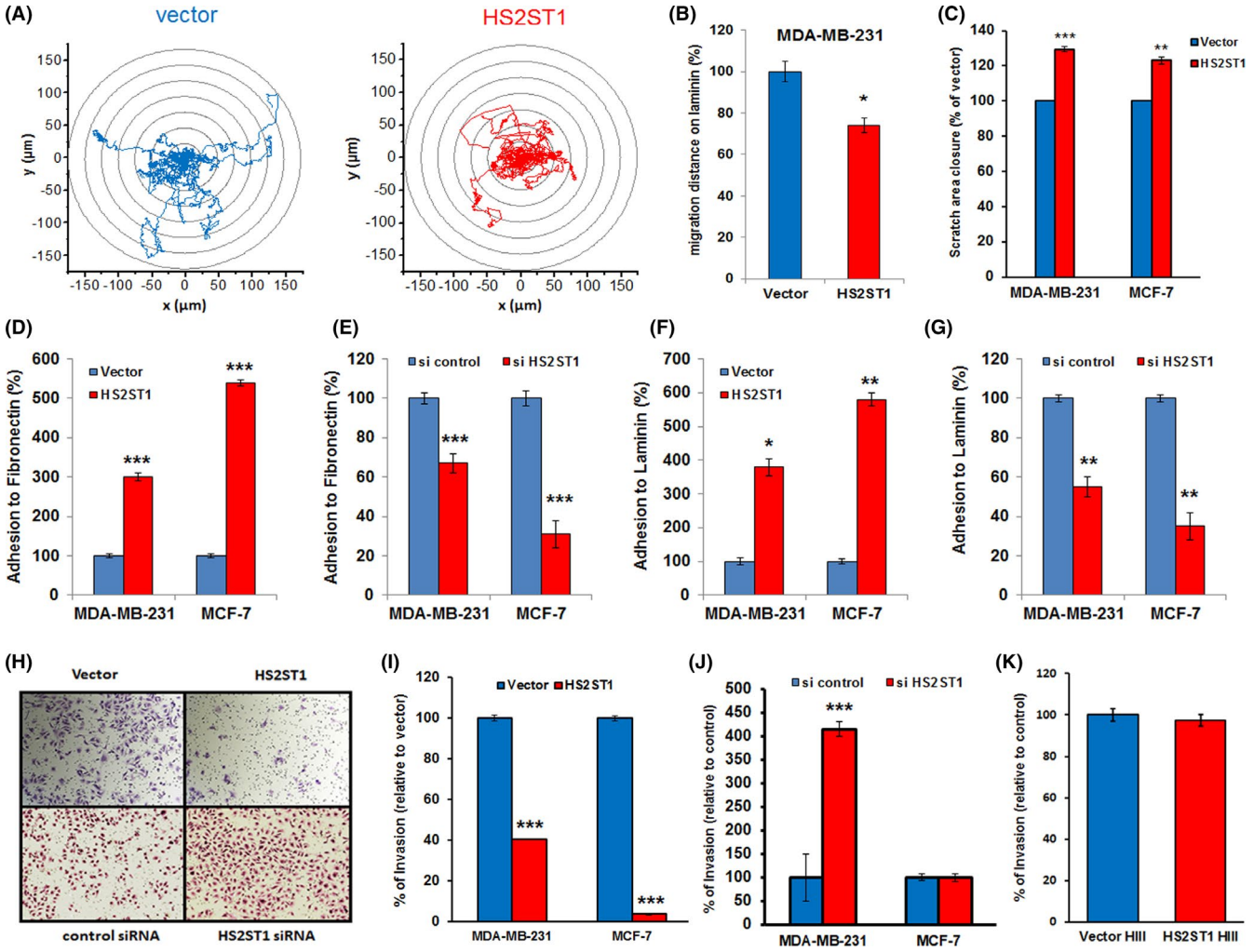

FIGURE 2 *HS2ST1* modulates breast cancer cell adhesion, migration and invasion. A, B, DHM time lapse analysis reveals lower migration of *HS2ST1*-transfected MDA-MB-231 cells (n = 13) compared with vector controls (n = 16), on laminin coating. A, Migration tracks. B, Quantification revealing a *c*. 30% decrease in the migration distance. N = 3, error bars = SEM. C, Scratch wound closure assay reveals slower migration of *HS2ST1*-transfected MDA-MB-231 and MCF-7 cells compared with controls. ***$P < .001$, **$P < .01$; $N \geq 9$, error bars = SEM. D-G, Cell adhesion to fibronectin and laminin is increased upon *HS2ST1* overexpression (D, F) and decreased upon *HS2ST1* depletion (E, G). N = 18, Error bars = SEM, ***$P < .001$, **$P < .01$, *$P < .05$. H-K, Impact of *HS2ST1* on invasive behavior of breast cancer cells in Matrigel invasion chamber assays. H, Representative images of Matrigel matrix filters. t = 24 h (highly invasive MDA-MB-231), t = 48 h (low invasive MCF-7). I, *HS2ST1* overexpression significantly inhibits invasion. J, siRNA knockdown of *HS2ST1* promotes MDA-MB-231 invasiveness, while invasion is not affected in MCF-7 cells. ***$P < .001$, **$P < .01$, $N \geq 6$, error bars = SEM. K, Vector controls and *HS2ST1*-overexpressing MDA-MB-231 cells displayed no difference in their invasion capacity upon prior HS degradation with 0.5 U/mL heparin lyase III (4 h). N = 6, error bars = SEM

3.3 | *HS2ST1* modulates breast cancer cell migration, cell-ECM adhesion, and invasiveness

Migration and cell-ECM adhesion are critical steps during cancer cell invasion that are regulated by HSPGs.[25,35,36] Hence, we tracked the migratory behavior of *HS2ST1*-overexpressing MDA-MB-231 cells by time lapse microscopy and observed a decrease in their capability to migrate on laminin by ~25% (Figure 2A,B). These results were consistent with data obtained by scratch wound assay, where *HS2ST1*-overexpressing cells displayed a significant delay of 23%-30% in wound closure (Figure 2C and Figure S1B). In vitro adhesion assays revealed that *HS2ST1*-overexpressing MDA-MB-231 cells showed significantly increased adhesion of 3.0-fold to fibronectin and ~3.8-fold to laminin, while MCF-7 showed a ~5.4-fold increase toward fibronectin compared with ~5.7-fold toward laminin substrate (Figure 2D-G). In contrast, *HS2ST1*-depleted MDA-MB-231 cells displayed a 33% decrease in adhesiveness to fibronectin and ~45% decrease to laminin compared with the controls (Figure 2E,G). The effect was more pronounced in MCF-7 cells, where a decrease of 70% to fibronectin and 66% to laminin was observed (Figure 2E,G). We next investigated the cellular capacity to invade through Matrigel, a basement membrane-like ECM. While invasion decreased in *HS2ST1*-overexpressing MCF-7 cells and in the highly metastatic MDA-MB-231 cells (Figure 2H,I), it dramatically increased upon *HS2ST1* knockdown in MDA-MB-231 (Figure 2H,J). In contrast, siRNA knockdown of *HS2ST1* in MCF-7 cells did not affect invasiveness (Figure 2J). We no

longer observed a difference in the invasive potential of control and *HS2ST1*-overexpressing cells after HS digestion with heparin lyase III, suggesting that indeed the HS and its modification correlate to the observed invasive phenotype (Figure 2K).

3.4 | *HS2ST1* overexpression reduces breast cancer cell viability and signal transduction via multiple pathways

HSPGs play an important role as signaling co-receptors.[1,2,7,37,38] To test the impact of altered *HS2ST1* expression, cell viability was assessed by MTT assay over a time course of 72 h (Figure 3A). While cell viability was consistently decreased upon *HS2ST1* overexpression in both cell lines at all timepoints after 24, 48 and 72 h, respectively, MDA-MB-231 cells were more strongly affected by *HS2ST1* overexpression compared with MCF-7 cells (Figures 3A and S1C). The *HS2ST1*-dependent decrease in viability was not due to increased apoptosis, as flow cytometric analysis of annexin V binding did not reveal significant differences between *HS2ST1*-overexpressing and control breast cancer cells (Figure S1D). Phosphokinase array screening revealed a net overall decrease in the phosphorylation status upon overexpression of *HS2ST1* in MDA-MB-231 cells. Phosphorylation of p38 MAPK, Erk 1/2 (p44/42 MAPK), JNK 1/2/3, EGFR, Akt, and p53, along with several other proteins, was decreased in *HS2ST1*-overexpressing compared with control cells, (Figure 3B and Table 2), indicating an important general role of *HS2ST1* in signal transduction. *HS2ST1* overexpression led to decreased activation of the p44/42 and p38 MAPK signaling pathways (Figures 3C,D and S1E,F) in MDA-MB-231 cells. *HS2ST1* knockdown resulted in similar constitutive activation levels of p44/42 MAPK in control and *HS2ST1*-overexpressing MDA-MB-231 cells (Figure 3E). In contrast, siRNA knockdown of *HS2ST1* activated p44/42 MAPK signaling in MCF-7 cells (Figure 3F).

3.5 | Alterations in the migratory and invasive behavior are associated with changes in the expression of the cell-cell adhesion molecule E-cadherin and the transcription factor TCF-4

The prognostically relevant cell-cell adhesion molecule E-cadherin is co-expressed with the HSPG Syndecan-1 in early breast cancer and

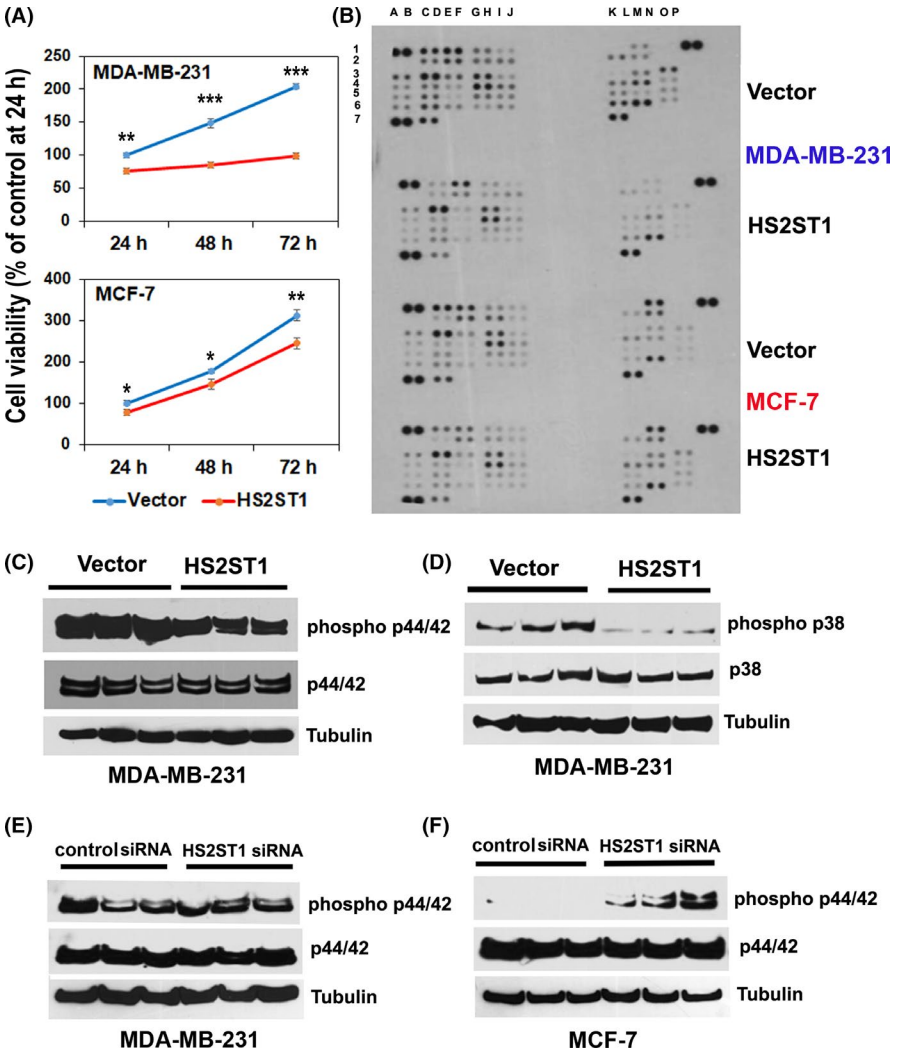

FIGURE 3 *HS2ST1* affects cell viability and modulates multiple signaling pathways. A, *HS2ST1* upregulation significantly reduces cell viability over a time course of 24-72 h (MTT assay), having a stronger impact in MDA-MB-231 cells compared with MCF-7 cells. $^{*}P < .05$, $^{**}P < .01$, $^{***}P < .001$, N = 6, error bars = SEM. B, Phosphokinase array blot showing an overall decrease in signaling upon *HS2ST1* overexpression compared with controls. C, D, Western blot analysis reveals that constitutive p44/42 (C) and p38 (D) MAPK activation were decreased in *HS2ST1*-overexpressing MDA-MB-231 cells. E, Basal p44/42 MAPK was activated upon *HS2ST1* siRNA knockdown in MDA-MB-231 cells raising the activation levels similar to the controls. F, siRNA knockdown of *HS2ST1* activates basal MAPK in MCF-7 cells compared with controls where the pathway is not active. Tubulin was used as a loading control. N = 9

TABLE 2 Relative activation of kinases and signaling receptors in HS2ST1 and control vector-transfected cell lines according to phosphokinase array screening

			HS2ST1-overexpressing cells	
Number	Protein	Phosphorylation site	MDA-MB 231	MCF-7
1 C,D	p 38 alpha	T180/Y182	Down	Down
1 E,F	ERK 1/2	T202/Y204, T185/Y187	Down	Down
1 G,H	JNK 1/2/3	T183/Y185, T221/Y223	Down	Down
2 C,D	EGFR	Y1086	Down	Down
2 E,F	Msk 1/2	S376/S360	Down	Down
2 G,H	AMPKα1	T183	Down	Down
2 I,J	Akt 1/2/3	S473	Down	No change
2 K,L	Akt 1/2/3	T308	Down	No change
2 M,N	P53	S46	Down	Slightly down
3 A,B	TOR	S2448	Slightly down	No change
3 E,F	HSP27	S78/S82	Down	Slightly down
3 G,H	AMPKα2	T172	Slightly down	No change
3 I,J	β-Catenin	—	Down	Slightly down
3 K,L	P70 S6 kinase	T389	Down	No change
3 M,N	P53	S15	Down	Slightly up
3 O,P	c-Jun	S63	Down	Up
4 A,B	Src	Y419	Slightly down	Slightly down
4 C,D	Lyn	Y397	Down	No change
4 E,F	Lck	Y394	Down	No change
4 G,H	Stat2	Y689	Slightly down	No change
4 I,H	Stat 5a	Y694	Down	Slightly down
4 K,L	P70 S6 kinase	T421/S424	Down	Slightly up
4 M,N	RSK 1/2/3	S380/S386/S377	Down	Slightly up
4 O,P	eNOS	S1177	Down	No change
5 A,B	Fyn	Y420	Down	No change
5 C,D	Yes	Y426	Down	No change
5 G,H	Stat 6	Y641	Down	Down
5 I,J	Stat 5B	Y699	Down	Down
5 K,L	Stat 3	Y705	Down	Slightly down
5 M,N	P27	T198	No change	Not expressed
5 O,P	PLC-γ1	Y783	Down	Slightly up
6 A,B	Hck	Y411	Down	Slightly down
6 C,D	Chk-2	T68	Down	No change
6 E,F	FAK	Y397	Slightly down	No change
6 G,H	Stat 5 a/b	Y694/Y699	Down	No change
6 K,L	Stat 3	S727	Down	No change
6 M,N	Wnk 1	T60	Down	No change
6 O,P	Pyk 2	Y402	Down	No change
7 C,D	PRAS 40	T246	Down	Down

regulates the invasive capability of cells.[39-42] While E-cadherin expression was increased in *HS2ST1*-overexpressing cells compared with controls, its expression was downregulated upon *HS2ST1* knockdown in both cell lines (Figure 4A-D). HSPGs modulate the Wnt/β-catenin signaling pathway, which regulates cell survival, proliferation, and differentiation.[43,44] Western blot analysis of the Wnt effector Tcf4 (Tcf7l2) confirmed strong downregulation in *HS2ST1*-overexpressing MDA-MB-231 and MCF-7 cells compared with controls (Figure 4E,F). Pharmacological inhibition of constitutive MAPK signaling in MDA-MB-231 cells expressing a different HS sulfotransferase,

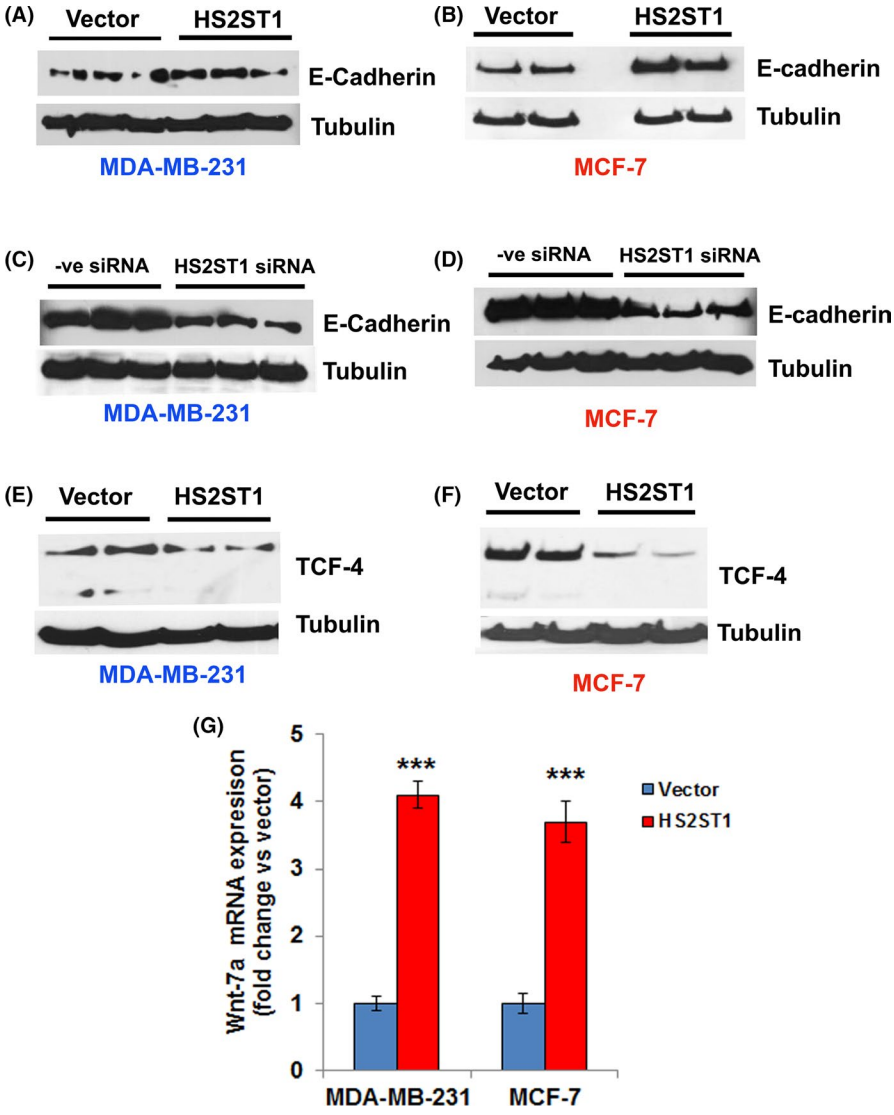

FIGURE 4 *HS2ST1* expression affects the expression of E-cadherin, Tcf4, and Wnt 7a. A, B, Western blot shows increased E-cadherin expression upon *HS2ST1* overexpression. C, D, *HS2ST1* siRNA knockdown decreases E-cadherin expression. E, F, *HS2ST1* overexpression leads to decreased expression of the Wnt-related transcription factor Tcf4. G, qRT-PCR reveals upregulation of *WNT-7a* in *HS2ST1*-overexpressing cells. ***$P < .001$, $N \geq 6$, error bars = SEM

HS3ST2, abolished the increased Tcf4 expression,[45] suggesting a cross-talk between the 2 pathways. Moreover, *HS2ST1* overexpression led to elevated Wnt 7a mRNA expression (Figures 4G and S1G).

3.6 | *HS2ST1* regulates the expression of epidermal growth factor receptor

EGFR expression is frequently elevated in breast cancer,[46] and its activation was affected by *HS2ST1* according to our phosphokinase array screening. qPCR analysis revealed a significant decrease in EGFR mRNA expression levels in *HS2ST1*-overexpressing cells while we observed an increased EGFR mRNA expression upon *HS2ST1* knockdown (Figures 5A,B and S1H). These data were confirmed at the protein level by western blot analysis (Figure 5C,D). We next tested if altered expression of *HS2ST1* affected the activation of MAPK signaling in the presence of specific growth factors. For this purpose, serum-starved *HS2ST1*-overexpressing MDA-MB-231 cells were stimulated with EGF, which resulted in a moderate increase in MAPK activation due to the known constitutive activation status[45] in this cell line (Figure 5E). In *HS2ST1*-overexpressing cells, constitutive and early EGF-induced MAPK activation were reduced compared with controls (Figure 5E). In MCF-7 cells, where the pathway is not constitutively active,[45] EGF activated p44/42 MAPK after 5 min of stimulation, whereas MAPK activation was reduced in *HS2ST1*-overexpressing cells (Figure 5F).

3.7 | Increased 2-*O*-sulfation affects binding of FGF-2 to HS and FGF-2-induced p44/42 MAPK activation

In breast and colon cancer, HSPGs modulate basic fibroblast growth factor (FGF-2)-mediated MAPK signaling.[25,46] FGF-2 signaling is effectively inhibited by 2-*O*- and *N*-sulfated HS oligosaccharides competing with cellular HS for binding to FGF-2.[47-49] In light of these findings, binding of FGF-2 to control and *HS2ST1*-overexpressing cells was analyzed by flow cytometry by in vitro binding of fluorescently labeled FGF-2. The results were comparable as the *HS2ST1*-overexpressing cells showed in both cell lines a ~20% reduced weaker binding of FGF-2 to HS compared with the controls (Figure 6A). Stimulation of *HS2ST1*-overexpressing

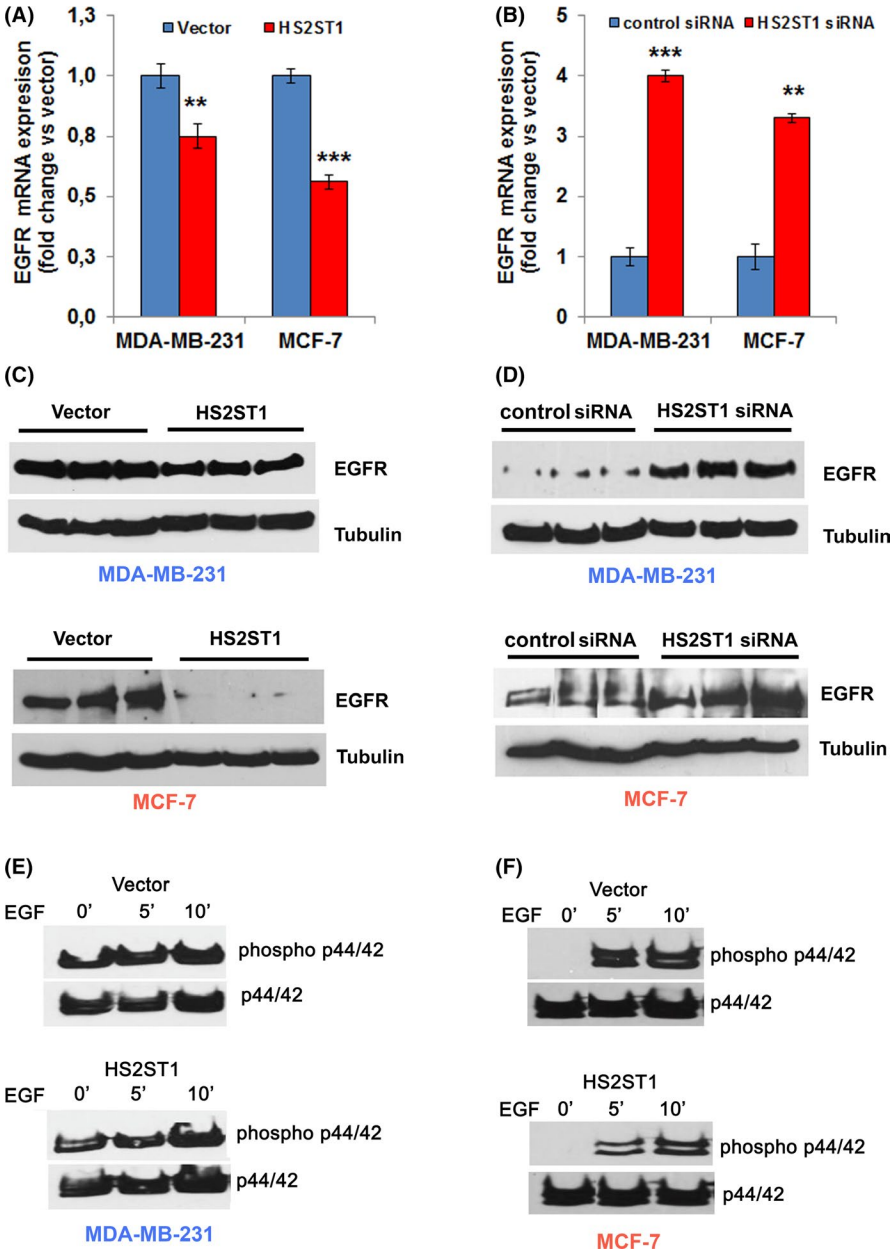

FIGURE 5 *HS2ST1* modulates EGFR expression and growth factor-mediated activation of p44/42 MAPK in breast cancer cells. A, qRT-PCR reveals downregulation of *EGFR* mRNA expression level in *HS2ST1*-overexpressing breast cancer cells. B, *HS2ST1* siRNA knockdown upregulates *EGFR* mRNA expression. ***$P < .001$, **$P < .01$, $N \geq 6$, error bars = SEM. C, Western blot showing decreased EGFR protein expression compared with controls in *HS2ST1*-overexpressing cell lines (upper panels), whereas EGFR expression is increased upon *HS2ST1* siRNA knockdown (D). E, F, *HS2ST1*-overexpressing MCF-7 cells show a decreased response to EGF stimulation. Serum-starved vector and *HS2ST1*-transfected cells were stimulated with 100 ng/mL EGF for 0, 5, and 10 min. Here, 25 μg of cell lysate/lane were analyzed by western blotting for phospho-p44/42 MAPK, p44/42 MAPK, and the loading control α-tubulin. Compared to controls, EGF treatment slightly decreased p44/42 MAPK activation as a readout of EGF-induced signaling in *HS2ST1*-overexpressing MCF-7 cells. The signaling response was attenuated to a lower extent in *HS2ST1*-overexpressing MDA-MB-231 cells

MDA-MB-231 cells with FGF-2 resulted in a weaker activation of the p44/42 MAPK signaling pathway compared with control cells (Figure 6B). In MCF-7 cells, FGF-2 activated the MAPK signaling in both control and *HS2ST1*-overexpressing cells, yet, the overall activation status of *HS2ST1*-overexpressing cells was lower than the controls (Figure 6B). To link the observed alterations in growth factor binding and mitogenic signaling to the phenotypic changes induced by altered *HS2ST1* expression, we evaluated cell viability and scratch wound repair in the absence or presence of the MAPK pathway (MEK1/MEK2) inhibitor U0126. siRNA depletion of HS2ST1 resulted in increased viability of MDA-MB-231 (Figure 6C) and MCF-7 cells (Figure 6D), which was reduced to control levels by U0126, suggesting a role for MAPK signaling in the *HS2ST1*-dependent process. In addition, MAPK inhibition generated a phenocopy of the delay in scratch wound motility observed in *HS2ST1*-overexpressing MDA-MB-231 cells (Figure 6E). Overall, these results indicated that altered cell behavior in *HS2ST1*-misexpressing breast cancer cells is associated with altered ligand binding and cellular signaling.

4 | DISCUSSION

In this report we demonstrate a novel role for *HS2ST1* in modulating breast cancer cell invasiveness via central signaling pathways including MAPK and Wnt (Figure 6F). Our findings are in line with studies in glioma, indicating a downregulation of *HS2ST1* and other HS sulfotransferases.[50] Mechanistically, HSPGs modulate MAPK signaling, promoting proliferation, migration, and invasion.[45,51-53] In our model cell lines, this pathway is constitutively active in MDA-MB-231 cells, but not in MCF-7.[51,54] Phosphorylation of Erk 1/2 (p44/42 MAPK) was less evident in *HS2ST1*-overexpressing MDA-MB-231 cells

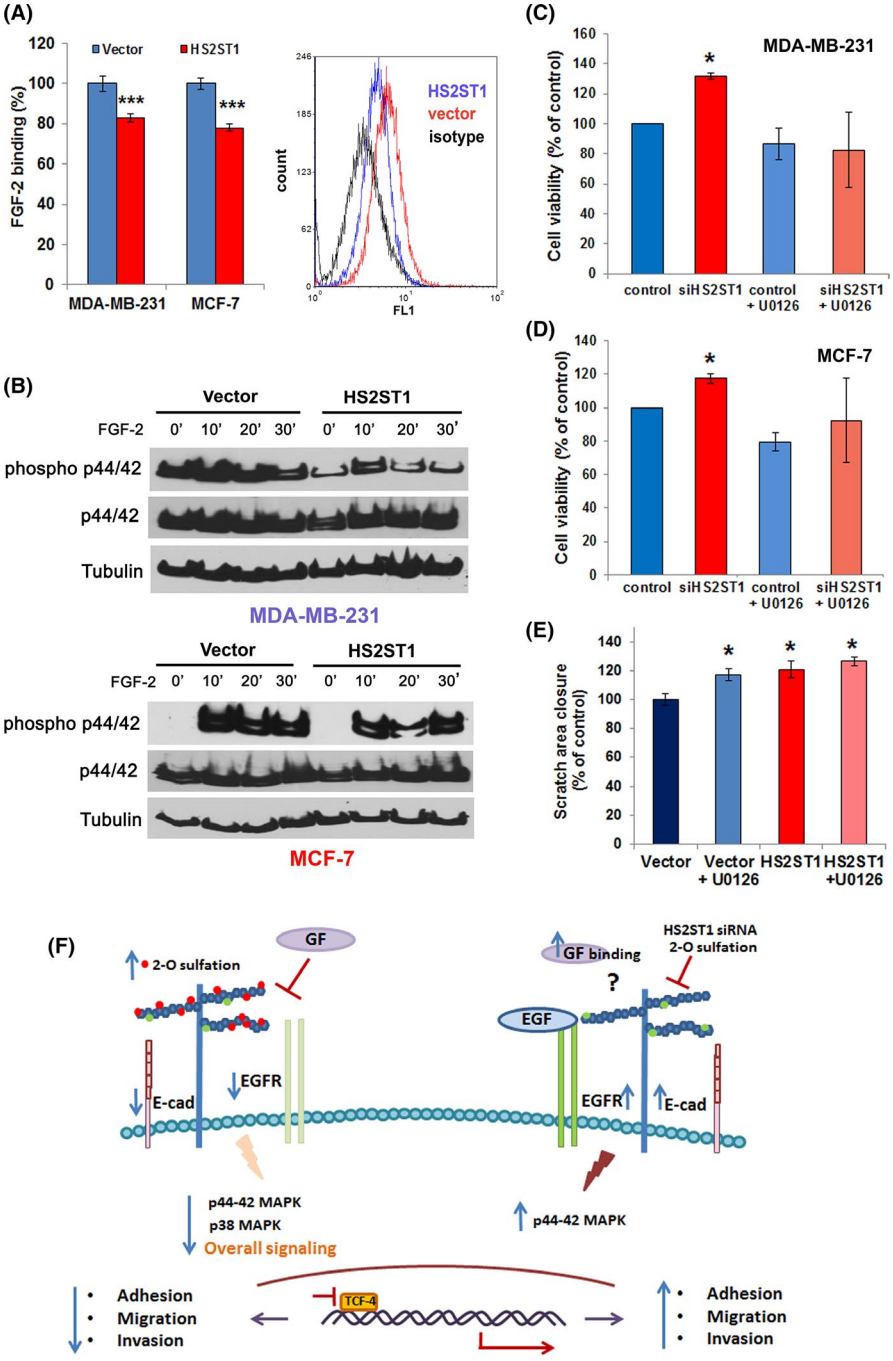

FIGURE 6 Altered *HS2ST1* expression affects FGF-2 binding, FGF-2-induced MAPK signaling, and MAPK-dependent cell viability and migration. A, *HS2ST1*-overexpressing breast cancer cells show reduced cell surface binding of biotinylated FGF-2. Flow cytometry, reveals a decrease of 20% and 30% in the binding efficiency of FGF-2 to *HS2ST1*-overexpressing MDA-MB-231 and MCF-7 cells compared with controls. Right panel, representative measurement (MCF-7 cells). ***$P < .001$, N = 3, error bars = SEM. B, *HS2ST1*-overexpression attenuates FGF-2-induced MAPK activation. Serum-starved vector and *HS2ST1*-transfected cells were stimulated with 20 ng/mL FGF-2 for a 0-30 min time course and 25 μg of cell lysate/lane were analyzed by western blotting for phospho-p44/42, p44/42 and the loading control α-tubulin. C, D, *HS2ST1* siRNA knockdown enhances breast cancer cell viability in an MAPK-dependent manner. MDA-MB-231 (C) and MCF-7 (D) cells were subjected to control or *HS2ST1* siRNA treatment in the absence or presence of the MAPK inhibitor U0126. While *HS2ST1* siRNA knockdown significantly enhanced breast cancer cell viability, this effect could be reduced to control levels by MAPK inhibition. *$P < .05$, N = 6, error bars = SEM. E, *HS2ST1* overexpression and MAPK inhibition by the MAPK inhibitor U0126 delay scratch wound repair in MDA-MB-231 cells. MAPK inhibition generates a phenocopy of *HS2ST1* overexpression. *$P < .05$, N ≥ 3, error bars = SEM. F, Model of the tumor-suppressive role of HS2ST1 in breast cancer. High levels of HS2ST1 resulted in structural changes in HS and altered growth factor binding, which resulted in attenuated signaling through the MAPK and additional pathways. Reduced signaling and expression of E-cadherin and EGFR was associated with reduced viability, adhesion, migration, and invasion of breast cancer cells

compared with the controls, correlating with the reduced invasive phenotype. In MDA-MB-231 cells, knockdown of *HS2ST1* did not result in a further increase in p44/42 MAPK activation, possibly because this pathway is already strongly constitutively active in these cells.[54] In contrast, in MCF-7 cells, *HS2ST1* knockdown was sufficient to activate this pathway, possibly because altered HS sulfation may have affected the binding and presentation of mitogens to a broad range of receptors, thus acting as a co-receptor and enhancing signaling through the MAPK pathway upon ligand engagement.[1,2,4] Surprisingly, siRNA knockdown of *HS2ST1* did not enhance invasiveness of MCF-7 cells in our Matrigel chamber assay. It has been shown that stimulation of MCF-7 cells with growth factors such as TGF-α only leads to transient activation of MAPK signaling and cell migration, whereas the same induces sustained MAPK activation, enhanced cell motility, and increased in vitro invasion of MDA-MB-231 cells,[51] which may be an underlying cause for our observation. Another MAPK, p38, was also less activated in *HS2ST1*-overexpressing MDA-MB-231 cells supporting the observed phenotype. Intriguingly, phosphokinase array data revealed an overall *HS2ST1*-dependent decrease in the phosphorylation status of p38, Erk 1/2, EGFR, Akt, JNK and several other proteins (see Table 2). The reduced overall signaling is in accordance with the observed decreased invasiveness of *HS2ST1*-overexpressing cells. EGFR, known to be overexpressed and activated in approximately 20%-25% of cancers,[55] acts as a central point for the activation and crosstalk with many signaling pathways relevant to tumor migration and invasion.[56] MAPK and other kinases like phosphatidylinositol-3-kinase (PI3-K) act downstream of EGFR activation, promoting tumor cell migration and invasion.[50,57-59] In addition, decreased activation or inhibition of p38 MAPK decreases breast cancer metastasis.[60]

Altered MAPK activation resulted in decreased expression of the Wnt pathway-related transcription factor Tcf4 (Tcf7/l2) in *HS2ST1*-overexpressing MDA-MB-231 cells. Indeed, a HS-dependent crosstalk between Wnt and MAPK pathways modulates invasiveness via regulation of several downstream targets such as proteases, cadherins, and ECM components.[45] Apart from Tcf4, Wnt 7a was transcriptionally upregulated in *HS2ST1*-overexpressing cells. Wnt signaling has been linked to the mammalian target of rapamycin (mTOR) pathway,[61] which promotes cancer cell invasion.[62] Notably, reduced mTOR signaling is associated with increased hormone resistance in MCF-7 cells,[63] while MAPK pathway activation may enhance the sensitivity of these cells to estradiol.[64] As the triple-negative cell line MDA-MB-231 does not express estrogen receptor alpha, differential activation of these pathways may have contributed to the partially divergent impact of *HS2ST1* on hormone receptor-positive and hormone receptor-negative cells. Previous studies have demonstrated the positive regulation of E-cadherin expression by Wnt 7a in lung cancer cells.[65] E-cadherin acts as a tumor suppressor because of its role in establishing cell-cell adhesion[66] and is known to be co-expressed along with syndecan-1 HSPG in early stages of breast cancer.[42] Here, we show that *HS2ST1* overexpression directs upregulation of E-cadherin, thereby establishing cell-cell adhesion, while the knockdown suppresses its expression, which is associated with cancer progression and metastasis.[67] Upregulation of E-cadherin in *HS2ST1*-overexpressing MCF-7 cells may have also had an impact on Tcf-4, as the cytoplasmic domains of E-cadherin bind to beta-catenin,[68] which would then not be available to activate Tcf-4. Notably, decreased E-cadherin expression and loss of cell-cell adhesion were also observed in *HS2ST1* morphant cells of zebrafish embryos.[69] Reduction of cell-cell adhesion is accompanied by decreased cell adhesion to ECM ligands[70] and it is known that cell-cell and cell-matrix adhesion directly determine cell motility.[2,35] We show a crucial role of *HS2ST1* in modulating cell-ECM adhesion as tumor cell-matrix adhesion is considered to be a key event regulating metastasis.[36,71] Increased binding of *HS2ST1*-overexpressing cells to fibronectin and laminin correlates with the observed migration and invasion phenotypes suggesting that the altered surface structure (as determined by FTIR analysis) reduces ECM adhesion, thereby facilitating cell migration. This finding is supported by a previous study in which increased adhesion to laminin inhibited cell movement.[72]

EGFR, one of the major upstream modulators of MAPK pathway is often overexpressed in more aggressive triple-negative breast cancers[46] and is associated with poor prognosis and large tumor size.[73,74] EGFR acts as a central point for many signaling pathways, including G-protein coupled receptor signaling, which transactivates EGFR, inducing invasion.[75,76] It regulates epithelial-to-mesenchymal transition via its downstream regulator-ERK inducing mesenchymal motility and invasion in cancer cells.[77] The *HS2ST1*-dependent changes in EGFR expression contribute to changes in invasive behavior of triple-negative MDA-MB-231 cells.

Previous studies have demonstrated that HS modulates signaling by growth factor binding[25,49] and that 2-*O*-sulfated HS oligosaccharides effectively bind to FGF-2.[47] It has been shown that HS, which binds to FGF but does not bind to the fibroblast growth factor receptor (FGFR), acts as a competitor.[17] We could demonstrate weaker binding of FGF-2 to *HS2ST1*-overexpressing cells, which may be one of the reasons for the observed reduction in signaling in these cells.[78,79] Moreover, the formation of FGF-FGFR signaling complexes is generally believed to be promoted by HS chains that bind to both growth factors and receptors.[80,81] The smaller effect of FGF-2 binding to cell surface HS compared with control cells could be due to steric hindrance of HS on the cell surface and/or to a conformational change in HS,[82] compared with isolated HS, for which binding sites are more freely available. Mechanistically, this explains the overall phenotypic end points obtained as a result of modifying HS specifically at the 2-*O* position.

A novel and non-invasive approach for analyzing sulfated GAGs from CM led to good discrimination between control and *HS2ST1*-overexpressing cells. By focusing the analysis on the sulfate absorption region, *HS2ST1*-transfected cell CM was different from the control counterparts both for MDA-MB-231 and MCF-7 cells, although more marked for MDA-MB-231. This suggests that an FTIR spectroscopic approach could be used as a rapid monitoring method for screening CM.

In conclusion, this study provides evidence for the promising role of *HS2ST1* in modulating breast cancer cell invasiveness via modulating EGFR and additional signaling pathways (Figure 6F). This report is the first to reveal the impact of an HS modifier enzyme, *HS2ST1*, in controlling the invasiveness of breast cancer cells in vitro. Further in vivo and clinical studies in this direction will be of great interest and importance for future potential cancer therapeutics.

ACKNOWLEDGMENTS

The authors thank Birgit Pers, Luisa Pohl, and Steffi Ketelhut for expert technical assistance, Dorothe Spillmann for performing GAG Disaccharide analysis, Mariana Stelling for kind assistance with HS purification, and Stephanie Beel for assistance with inhibitor studies. Funding was provided by Deutsche Forschungsgemeinschaft DFG IRTG "Molecular and Cellular GlycoSciences" Grant GRK 1549 (to AVK, SKK, FMG and MG), Deutscher Akademischer Austauschdienst DAAD Grant PROBRAL 54387857 (to MG and MSGP), and a WWU fellowship of the University of Münster (to JMM).

DISCLOSURE

The authors have no conflict of interest.

ORCID

Stéphane Brézillon https://orcid.org/0000-0001-7954-8340
Valérie Untereiner https://orcid.org/0000-0002-3360-0171
Ganesh Dhruvananda Sockalingum https://orcid.org/0000-0003-3160-4678
Hossam Taha Mohamed https://orcid.org/0000-0003-1989-5783
Björn Kemper https://orcid.org/0000-0003-3693-9397
Benedikt Mohr https://orcid.org/0000-0001-9769-9986
Sherif Abdelaziz Ibrahim https://orcid.org/0000-0001-6403-7345
Francisco M. Goycoolea https://orcid.org/0000-0001-7949-5429
Mauro S.G. Pavão https://orcid.org/0000-0002-1336-4271
Juliana M. Motta https://orcid.org/0000-0001-6687-6222
Martin Götte https://orcid.org/0000-0003-2360-2496

REFERENCES

1. Bernfield M, Götte M, Park PW, et al. Functions of cell surface heparan sulfate proteoglycans. *Annu Rev Biochem*. 1999;68:729-777.
2. Karamanos NK, Piperigkou Z, Theocharis AD, et al. Proteoglycan chemical diversity drives multifunctional cell regulation and therapeutics. *Chem Rev*. 1999;118:9152-9232.
3. Häcker U, Nybakken K, Perrimon N. Heparan sulphate proteoglycans: the sweet side of development. *Nat Rev Mol Cell Biol*. 2005;6:530-541.
4. Espinoza-Sánchez NA, Götte M. Role of cell surface proteoglycans in cancer immunotherapy. *Semin Cancer Biol*. 2020;62:48-67.
5. Blackhall FH, Merry CLR, Davies EJ, Jayson GC. Heparan sulfate proteoglycans and cancer. *Br J Cancer*. 2001;85:1094-1098.
6. Sasisekharan R, Shriver Z, Venkataraman G, Narayanasami U. Roles of heparan-sulfate glycosaminoglycans in cancer. *Nat Rev Cancer*. 2002;2:521-528.
7. Hassan H, Greve B, Pavão MS, Kiesel L, Ibrahim SA, Götte M. Syndecan-1 modulates β-integrin-dependent and interleukin-6-dependent functions in breast cancer cell adhesion, migration, and resistance to irradiation. *FEBS J*. 2013;280:2216-2227.
8. Lindahl U, Gullberg KM, Kjellen L. Regulated diversity of heparan sulfate. *J Biol Chem*. 1998;273:24979-24982.
9. Gallagher JT. Multiprotein signaling complexes: regional assembly on heparan sulphate. *Biochem Soc Trans*. 2006;34:438-441.
10. Nakato H, Kimata K. Heparan sulfate fine structure and specificity of proteoglycan functions. *Biochim Biophys Acta*. 2002;1573:312-318.
11. Dejima K, Takemura M, Nakato E, et al. Analysis of Drosophila glucuronyl C5-epimerase: implications for developmental roles of heparan sulfate sulfation compensation and 2-*O*-sulfated glucuronic acid. *J Biol Chem*. 2013;288:34384-34393.
12. Esko JD, Selleck SB. Order out of chaos: assembly of ligand binding sites in heparan sulfate. *Annu Rev Biochem*. 2002;71:435-471.
13. Pinhal MA, Smith B, Olson S, Aikawa J, Kimata K, Esko JD. Enzyme interactions in heparan sulfate biosynthesis: uronosyl 5-epimerase and 2-*O*-sulfotransferase interact in vivo. *Proc Natl Acad Sci*. 2001;98:12984-12989.
14. Esko JD, Lindahl U. Molecular diversity of heparan sulfate. *J Clin Invest*. 2001;108:169-173.
15. Robinson CJ, Mulloy B, Gallagher JT, Stringer SE. VEGF165-binding sites within heparan sulfate encompass two highly sulfated domains and can be liberated by K5 lyase. *J Biol Chem*. 2006;281:1731-1740.
16. Maccarana M, Casu B, Lindahl U. Minimal sequence in heparin/heparan sulfate required for binding of basic fibroblast growth factor. *J Biol Chem*. 1994;269:3903.
17. Guimond S, Maccarana M, Olwin BB, Lindahl U, Rapraeger AC. Activating and inhibitory heparin sequences for FGF-2 (basic FGF). *J Biol Chem*. 1993;268:23906-23914.
18. Smeds E, Feta A, Kusche-Gullberg M. Target selection of heparan sulfate hexuronic acid 2-*O*-sulfotransferase. *Glycobiology*. 2010;20:1274-1282.
19. Rong J, Habuchi H, Kimata K, Lindahl U, Kusche-Gullberg M. Substrate specificity of the heparan sulfate hexuronic acid 2-Osulfotransferase. *Biochemistry*. 2001;40:5548-5555.
20. Bullock SL, Fletcher JM, Beddington RS, Wilson VA. Renal agenesis in mice homozygous for a gene trap mutation in the gene encoding heparan sulfate 2-sulfotransferase. *Genes Dev*. 1998;12:1894-1906.
21. Kinnunen T, Huang Z, Townsend J, et al. Heparan 2-*O*-sulfotransferase, hst-2, is essential for normal cell migration in *Caenorhabditis elegans*. *Proc Natl Acad Sci*. 2005;102:1507-1512.
22. Afratis N, Gialeli C, Nikitovic D, et al. Glycosaminoglycans: key players in cancer cell biology and treatment. *FEBS J*. 2012;279:1177-1197.
23. Yip GW, Smollich M, Gotte M. Therapeutic value of glycosaminoglycans in cancer. *Mol Cancer Ther*. 2006;5:2139-2148.
24. Fuster MM, Esko JD. The sweet and sour of cancer: glycans as novel therapeutic targets. *Nat Rev Cancer*. 2005;5:526-542.
25. Nikolova V, Koo CY, Ibrahim SA, et al. Differential roles for membrane-bound and soluble syndecan-1 (CD138) in breast cancer progression. *Carcinogenesis*. 2009;30:397-407.
26. Ledin J, Staatz W, Li JP, et al. Heparan sulfate structure in mice with genetically modified heparan sulfate production. *J Biol Chem*. 2004;279:42732-42741.
27. Götte M, Mohr C, Koo CY, et al. miR-145-dependent targeting of junctional adhesion molecule A and modulation of fascin expression are associated with reduced breast cancer cell motility and invasiveness. *Oncogene*. 2010;29:6569-6580.
28. Kemper B, Carl D, Höink A, von Bally G, Bredebusch I, Schnekenburger J. Modular digital holographic microscopy system for marker free quantitative phase contrast imaging of living cells. *Proceedings of SPIE*. 2006;6191:T-1-T-8.
29. Kemper B, von Bally G. Digital holographic microscopy for life cell applications and technical inspection. *Appl Opt*. 2008;47:A52-A61.

30. Kemper B, Bauwens A, Vollmer A, et al. Label-free quantitative cell division monitoring of endothelial cells by digital holographic microscopy. *J Biomedical Optics*. 2010;153:036009.
31. Mohamed HT, Untereiner V, Sockalingum GD, Brézillon S. Implementation of infrared and Raman modalities for glycosaminoglycan characterization in complex systems. *Glycoconj J*. 2017;34:309-323.
32. Mainreck N, Brézillon S, Sockalingum GD, Maquart FX, Manfait M, Wegrowski Y. Characterization of glycosaminoglycans by tandem vibrational microspectroscopy and multivariate data analysis. *Methods Mol Biol*. 2012;836:117-130.
33. Mainreck N, Brézillon S, Sockalingum GD, Maquart FX, Manfait M, Wegrowski Y. Rapid characterization of glycosaminoglycans using a combined approach by infrared and Raman microspectroscopies. *J Pharm Sci*. 2011;100(2):441-450.
34. Brézillon S, Untereiner V, Lovergne L, et al. Glycosaminoglycan profiling in different cell types using infrared spectroscopy and imaging. *Anal Bioanal Chem*. 2014;406(24):5795-5803.
35. Weinberg R. *Moving Out: Invasion and Metastasis. The Biology of Cancer. Chapter 14*. New York, NY: Garland Science, Taylor & Francis Group, LLC; New York, NY; 2007:587-654.
36. Fidler IJ. Review: biologic heterogeneity of cancer metastases. *Breast Cancer Res Treat*. 1987;9:17-26.
37. Knelson EH, Nee JC, Blobe GC. Heparan sulfate signaling in cancer. *Trends Biochem Sci*. 2014;37:277-288.
38. Quarto N, Amalric F. Heparan sulfate proteoglycans as transducers of FGF-2 signaling. *J Cell Sci*. 1994;107:3201-3212.
39. Birchmeier W, Hülsken J, Behrens J. E-cadherin as an invasion suppressor. *Ciba Found Symp*. 1995;189:124-136.
40. Chen H, Paradies NE, Chaiken MF, Brackenbury R. E-cadherin mediates adhesion and suppresses cell motility via distinct mechanisms. *J Cell Sci*. 1997;110:345-356.
41. Parker C, Rampaul RS, Pinder SE, et al. E-cadherin as a prognostic indicator in primary breast cancer. *Br J Cancer*. 2001;85:1958-1963.
42. Götte M, Kersting C, Radke I, Kiesel L, Wülfing P. An expression signature of syndecan-1 (CD138), E-cadherin and c-met is associated with factors of angiogenesis and lymphangiogenesis in ductal breast carcinoma in situ. *Breast Cancer Res*. 2007;9:R8.
43. Miller JR, Hocking AM, Brown JD, Moon RT. Mechanism and function of signal transduction by the Wnt/beta-catenin and Wnt/Ca^{2+} pathways. *Oncogene*. 1999;18:7860-7872.
44. Liu BY, Kim YC, Leatherberry V, Cowin P, Alexander CM. Mammary gland development requires syndecan-1 to create a beta-catenin/TCF-responsive mammary epithelial subpopulation. *Oncogene*. 2003;22:9243-9253.
45. Vijaya Kumar AV, Salem Gassar E, Spillmann D, et al. HS3ST2 modulates breast cancer cell invasiveness via MAP kinase- and Tcf4 (Tcf7l2)-dependent regulation of protease and cadherin expression. *Int J Cancer*. 2014;135:2579-2592.
46. Burness ML, Grushko TA, Olopade OI. Epidermal growth factor receptor in triplenegative and basal-like breast cancer: promising clinical target or only a marker? *Cancer J*. 2010;16:23-32.
47. Ashikari-Hada S, Habuchi H, Sugaya N, Kobayashi T, Kimata K. Specific inhibition of FGF-2 signaling with 2-*O*-sulfated octasaccharides of heparan sulfate. *Glycobiology*. 2009;19:644-654.
48. Cole CL, Hansen SU, Baráth M, et al. Synthetic heparan sulfate oligosaccharides inhibit endothelial cell functions essential for angiogenesis. *PLoS One*. 2010;5:e11644.
49. Floer M, Götte M, Wild MK, et al. Enoxaparin improves the course of dextran sodium sulfate-induced colitis in syndecan-1-deficient mice. *Am J Pathol*. 2010;176:146-157.
50. Ushakov VS, Tsidulko AY, de La Bourdonnaye G, et al. Heparan sulfate biosynthetic system is inhibited in human glioma due to EXT1/2 and HS6ST1/2 down-regulation. *Int J Mol Sci*. 2017;18(11):2301.
51. Krueger JS, Keshamouni VG, Atanaskova N, Reddy KB. Temporal and quantitative regulation of mitogen-activated protein kinase (MAPK) modulates cell motility and invasion. *Oncogene*. 2011;20:4209-4218.
52. Roux PP, Blenis J. ERK and p38 MAPK-activated protein kinases: a family of protein kinases with diverse biological functions. *Microbiol Mol Biol Rev*. 2004;68:320-344.
53. Reddy KB, Krueger JS, Kondapaka SB, Diglio CA. Mitogen-activated protein kinase (MAPK) regulates the expression of progelatinase B (MMP-9) in breast epithelial cells. *Int J Cancer*. 1999;82:268-273.
54. Hoshino R, Chatani Y, Yamori T, et al. Constitutive activation of the 41-/43-kDa mitogen-activated protein kinase pathway in human tumors. *Oncogene*. 1999;18:813-822.
55. Earp HS III, Calvo BF, Sartor CI. The EGF receptor family– multiple roles in proliferation, differentiation, and neoplasia with an emphasis on HER4. *Trans Am Clin Climatol Assoc*. 2003;114:315-333.
56. Wang GK, Zhang W. The signaling network of tumor invasion. *Histol Histopathol*. 2005;20:593-602.
57. Price DJ, Avraham S, Feuerstein J, Fu Y, Avraham HK. The invasive phenotype in HMT-3522 cells requires increased EGF receptor signaling through both PI 3-kinase and ERK 1,2 pathways. *Cell Commun Adhes*. 2002;9:87-102.
58. Wan G, Wang F, Ding W, et al. APRIL induces tumorigenesis and metastasis of colorectal cancer cells via activation of the PI3K/Akt pathway. *PLoS One*. 2013;8:e55298.
59. Bellacosa A, Kumar CC, Di Cristofano A, Testa JR. Activation of AKT kinases in cancer: implications for therapeutic targeting. *Adv Cancer Res*. 2005;94:29-86.
60. Suarez-Cuervo C, Merrell MA, Watson L, et al. Breast cancer cells with inhibition of p38alpha have decreased MMP-9 activity and exhibit decreased bone metastasis in mice. *Clin Exp Metastasis*. 2004;21:525-533.
61. Park YL, Kim HP, Cho YW, et al. Activation of WNT/β-catenin signaling results in resistance to a dual PI3K/mTOR inhibitor in colorectal cancer cells harboring PIK3CA mutations. *Int J Cancer*. 2019;144:389-401.
62. Hsieh AC, Liu Y, Edlind MP, et al. The translational landscape of mTOR signalling steers cancer initiation and metastasis. *Nature*. 2012;485:55-61.
63. Leung EY, Kim JE, Askarian-Amiri M, Joseph WR, McKeage MJ, Baguley BC. Hormone resistance in two MCF-7 breast cancer cell lines is associated with reduced mTOR signaling, decreased glycolysis, and increased sensitivity to cytotoxic drugs. *Front Oncol*. 2014;4:221.
64. Yue W, Wang JP, Conaway M, Masamura S, Li Y, Santen RJ. Activation of the MAPK pathway enhances sensitivity of MCF-7 breast cancer cells to the mitogenic effect of estradiol. *Endocrinology*. 2002;143:3221-3229.
65. Ohira T, Gemmill RM, Ferguson K, et al. WNT7a induces E-cadherin in lung cancer cells. *PNAS*. 2003;100:10429-10434.
66. Christofori G, Semb H. The role of the cell-adhesion molecule E-cadherin as a tumor-suppressor gene. *Trends Biochem Sci*. 1999;24:73-76.
67. Weinberg R. *The Biology of Cancer*. New York, NY: Garland Science; 2006:864.
68. Loh CY, Chai JY, Tang TF, et al. The E-Cadherin and N-cadherin switch in epithelial-to-mesenchymal transition: signaling, therapeutic implications, and challenges. *Cells*. 2019;8:1118.
69. Cadwalader EL, Condic ML, Yost HJ. 2-O-sulfotransferase regulates Wnt signaling, cell adhesion and cell cycle during zebrafish epiboly. *Development*. 2012;139:1296-1305.
70. di Martino E, Kelly G, Roulson JA, Knowles MA. Alteration of cell-cell and cell-matrix adhesion in urothelial cells: an oncogenic mechanism for mutant FGFR3. *Mol Cancer Res*. 2015;13:138-148.

71. Paget S. The distribution of secondary growths in cancer of the breast. *Cancer Metastasis Rev*. 1989;8:98-101.
72. Guo Q, Xia B, Zhang F, et al. Tetraspanin CO-029 inhibits colorectal cancer celln movement by deregulating cell-matrix and cell-cell adhesions. *PLoS One*. 2012;7:e38464.
73. Sainsbury JR, Farndon JR, Needham GK, Malcolm AJ, Harris AL. Epidermal-growth-factor receptor status as predictor of early recurrence of and death from breast cancer. *Lancet*. 1987;1:1398-1402.
74. Ciardielloa F, Tortora G. Epidermal growth factor receptor (EGFR) as a target in cancer therapy: understanding the role of receptor expression and other molecular determinants that could influence the response to anti-EGFR drugs. *Eur J Cancer*. 2003;39:1348-1354.
75. Eccles SA. The epidermal growth factor receptor/Erb-B/HER family in normal and malignant breast biology. *Int J Dev Biol*. 2011;55:685-696.
76. Schafer B, Gschwind A, Ullrich A. Multiple G-protein coupled receptor signals converge on the epidermal growth factor receptor to promote migration and invasion. *Oncogene*. 2004;23:991-999.
77. Doehn U, Hauge C, Frank SR, et al. RSK is a principal effector of the RAS-ERK pathway for eliciting a coordinate promotile/invasive gene program and phenotype in epithelial cells. *Mol Cell*. 2009;35:511-522.
78. Xu R, Ori A, Rudd TR, et al. Diversification of the structural determinants of fibroblast growth factor–heparin interactions: implications for binding specificity. *J Biol Chem*. 2012;287:40061-40073.
79. Ori A, Free P, Courty J, Wilkinson MC, Fernig DG. Identification of heparin-binding sites in proteins by selective labeling. *Mol Cell Proteomics*. 2009;8:2256-2265.
80. Mohammadi M, Olsen SK, Ibrahimi OA. Structural basis for fibroblast growth factor receptor activation. *Cytokine Growth Factor Rev*. 2005;16:107-137.
81. Harmer NJ. Insights into the role of heparan sulphate in fibroblast growth factor signaling. *Biochem Soc Trans*. 2006;34:442-445.
82. Patel HV, Vyas AA, Vyas KA, et al. Heparin and heparan sulfate bind to snake cardiotoxin. Sulfated oligosaccharides as a potential target for cardiotoxin action. *J Biol Chem*. 1997;272:1484-1492.

SUPPORTING INFORMATION

Additional supporting information may be found online in the Supporting Information section.

How to cite this article: Vijaya Kumar A, Brézillon S, Untereiner V, et al. HS2ST1-dependent signaling pathways determine breast cancer cell viability, matrix interactions, and invasive behavior. *Cancer Sci*. 2020;111:2907–2922. https://doi.org/10.1111/cas.14539